

## $\beta$ -decay spectroscopy of neutron-rich $^{160,161,162}\text{Sm}$ isotopes

Z. Patel<sup>1,2,a</sup>, Zs. Podolyák<sup>1</sup>, P. M. Walker<sup>1</sup>, P. H. Regan<sup>1,3</sup>, P.-A. Söderström<sup>2</sup>, H. Watanabe<sup>2,4,5</sup>, E. Ideguchi<sup>6,7</sup>, G. S. Simpson<sup>8</sup>, S. Nishimura<sup>2</sup>, F. Browne<sup>2,10</sup>, P. Doornenbal<sup>2</sup>, G. Lorusso<sup>2,3</sup>, S. Rice<sup>1,2</sup>, L. Sinclair<sup>2,11</sup>, T. Sumikama<sup>12</sup>, J. Wu<sup>2,9</sup>, Z. Y. Xu<sup>13</sup>, N. Aoi<sup>6,7</sup>, H. Baba<sup>2</sup>, F. L. Bello Garrote<sup>14</sup>, G. Benzoni<sup>15</sup>, R. Daido<sup>7</sup>, Zs. Dombárdi<sup>22</sup>, Y. Fang<sup>7</sup>, N. Fukuda<sup>2</sup>, G. Gey<sup>8</sup>, S. Go<sup>16</sup>, A. Gottardo<sup>17</sup>, N. Inabe<sup>2</sup>, T. Isobe<sup>2</sup>, D. Kameda<sup>2</sup>, K. Kobayashi<sup>18</sup>, M. Kobayashi<sup>16</sup>, T. Komatsubara<sup>19,20</sup>, I. Kojouharov<sup>21</sup>, T. Kubo<sup>2</sup>, N. Kurz<sup>21</sup>, I. Kuti<sup>22</sup>, Z. Li<sup>23</sup>, H. L. Liu<sup>24</sup>, M. Matsushita<sup>16</sup>, S. Michimasa<sup>16</sup>, C.-B. Moon<sup>25</sup>, H. Nishibata<sup>7</sup>, I. Nishizuka<sup>12</sup>, A. Odahara<sup>7</sup>, E. Şahin<sup>14</sup>, H. Sakurai<sup>2,13</sup>, H. Schaffner<sup>21</sup>, H. Suzuki<sup>2</sup>, H. Takeda<sup>2</sup>, M. Tanaka<sup>7</sup>, J. Taprogge<sup>26,27</sup>, Zs. Vajta<sup>22</sup>, F. R. Xu<sup>9</sup>, A. Yagi<sup>7</sup>, and R. Yokoyama<sup>16</sup>

<sup>1</sup>Department of Physics, University of Surrey, Guildford, GU2 7XH, United Kingdom

<sup>2</sup>RIKEN Nishina Center, 2-1 Hirosawa, Wako-shi, Saitama 351-0198, Japan

<sup>3</sup>National Physical Laboratory, Teddington, Middlesex, TW11 0LW, United Kingdom

<sup>4</sup>International Research Center for Nuclei and Particles in the Cosmos, Beihang University, Beijing 100191, China

<sup>5</sup>School of Physics and Nuclear Energy Engineering, Beihang University, Beijing 100191, China

<sup>6</sup>Research Center for Nuclear Physics (RCNP), Osaka University, Ibaraki, Osaka 567-0047, Japan

<sup>7</sup>Department of Physics, Osaka University, Machikaneyama-machi 1-1, Osaka 560-0043 Toyonaka, Japan

<sup>8</sup>LPSC, Université Joseph Fourier Grenoble 1, CNRS/IN2P3, Institut National Polytechnique de Grenoble, F-38026 Grenoble Cedex, France

<sup>9</sup>School of Physics and State Key Laboratory of Nuclear Physics and Technology, Peking University, Beijing 100871, China

<sup>10</sup>School of Computing, Engineering and Mathematics, University of Brighton, Brighton, BN2 4JG, United Kingdom

<sup>11</sup>Department of Physics, University of York, Heslington, York, YO10 5DD, United Kingdom

<sup>12</sup>Department of Physics, Tohoku University, Aoba, Sendai, Miyagi 980-8578, Japan

<sup>13</sup>Department of Physics, University of Tokyo, Hongo, Bunkyo-ku, Tokyo 113-0033, Japan

<sup>14</sup>Department of Physics, University of Oslo, Oslo, Norway

<sup>15</sup>INFN Sezione di Milano, I-20133 Milano, Italy

<sup>16</sup>Center for Nuclear Study (CNS), University of Tokyo, Wako, Saitama 351-0198, Japan

<sup>17</sup>Instituto Nazionale di Fisica Nucleare, Laboratori Nazionali di Legnaro, I-35020 Legnaro, Italy

<sup>18</sup>Department of Physics, Rikkyo University, 3-34-1 Nishi-Ikebukuro, Toshima-ku, Tokyo 171-8501, Japan

<sup>19</sup>Research Facility Center for Pure and Applied Science, University of Tsukuba, Ibaraki 305-8577, Japan

<sup>20</sup>Rare Isotope Science Project, Institute for Basic Science, Daejeon 305-811, Korea

<sup>21</sup>GSI Helmholtzzentrum für Schwerionenforschung GmbH, 64291 Darmstadt, Germany

<sup>22</sup>Institute for Nuclear Research, Hungarian Academy of Sciences, P. O. Box 51, Debrecen, H-4001, Hungary

<sup>23</sup>School of Physics, Peking University, Beijing 100871, China

<sup>24</sup>Hoseo University, Asan, Chungnam 336-795, Korea

<sup>25</sup>Instituto de Estructura de la Materia, CSIC, E-28006 Madrid, Spain

<sup>26</sup>Departamento de Física Teórica, Universidad Autónoma de Madrid, E-28049 Madrid, Spain

**Abstract.** Neutron-rich  $^{160,161,162}\text{Sm}$  isotopes have been populated at the RIBF, RIKEN via  $\beta$  decay for the first time.  $\beta$ -coincident  $\gamma$  rays were observed in all three isotopes including  $\gamma$  rays from the isomeric decay of  $^{160}\text{Sm}$  and  $^{162}\text{Sm}$ . The isomers in  $^{160}\text{Sm}$  and  $^{162}\text{Sm}$  have previously been observed but have been populated via  $\beta$  decay for the first time. The isomeric state in  $^{162}\text{Sm}$  is assigned a  $4^- \nu_{7/2}^+ [633] \otimes \nu_{1/2}^- [521]$  configuration based on the decay pattern. The level schemes of  $^{160}\text{Sm}$  and  $^{162}\text{Sm}$  are presented. The ground states in the parent nuclei  $^{160}\text{Pm}$  and  $^{162}\text{Pm}$  are both assigned a  $6^- \nu_{7/2}^+ [633] \otimes \pi_{5/2}^- [532]$  configuration based on the population of states in the daughter nuclei. Blocked BCS calculations were performed to further investigate the spin-parities of the ground states in  $^{160}\text{Pm}$ ,  $^{161}\text{Pm}$ , and  $^{162}\text{Pm}$ , and the isomeric state in  $^{162}\text{Sm}$ .

## 1 Introduction

The  $\beta$  decay of neutron-rich nuclei can be a useful tool to probe low-lying states in nuclei that are otherwise diffi-

cult to populate. Here we present nuclear data on  $^{160}\text{Sm}$ ,  $^{161}\text{Sm}$ , and  $^{162}\text{Sm}$  that have been populated via  $\beta$  decay for the first time. These nuclei lie in the neutron-rich mid-shell region between the closed shells of  $Z = 50$  and  $82$  and  $N = 82$  and  $126$  and are expected to be among the most col-

<sup>a</sup>e-mail: z.patel@surrey.ac.uk

lective of nuclei. Therefore this is a good testing ground for collective models. Neutron-rich nuclei are created in the  $r$  process, which is responsible for the production of half the nuclei that exist with  $Z > 26$  (iron). There are three major peaks in the elemental abundances at  $A \approx 80$ , 130, and 195. These are due to the closed shells at  $N = 50$ , 82, and 126 that create “waiting” points in the  $r$  process [1]. Experimental data has led to an improved understanding of these peaks [2–4]. There is also a less pronounced peak at  $A \approx 160$ , of which the origin is not as clear. It is thought to be due to a deformation maximum [5], however recent theories [6, 7] and experimental data [8] have also suggested that a subshell gap at  $N = 100$  may play a role. Investigation of nuclei around  $A = 160$  may provide insight into the possible origins of this peak. The high intensity uranium beam at the RIBF, RIKEN has been utilised to populate these isotopes at the limits of known nuclei.

## 2 Experimental method

Neutron-rich  $^{160,161,162}\text{Pm}$  isotopes were produced by in-flight fission of a 345 A-MeV  $^{238}\text{U}$  beam with an average beam intensity of 10 particle-nA incident on a  $^9\text{Be}$  target at the RIBF. The secondary beam was passed through Bi-gRIPS and the ZeroDegree spectrometers [9, 10] where the nuclei were separated according to their mass-to-charge ratio ( $A/q$ ) and atomic number ( $Z$ ) using time-of-flight, magnetic rigidity and energy loss (TOF,  $B\rho$ , and  $\Delta E$ ) [11, 12].

The ions were implanted into an active stopper, WAS3ABi: Wide Angle Silicon-Strip-Stopper Array for Beta and ion detection [13]. This consisted of 5 DSSDs, each with 60 x 40 1-mm strips. A time window of 1 second was used to correlate an ion implantation with a  $\beta$ -decay particle detected in the same or neighbouring pixel. The  $\gamma$  rays emitted following  $\beta$  decay were detected using EURICA (Euroball-RIKEN Cluster Array) [14–16]: 84 HPGe crystals arranged in a  $4\pi$  configuration at  $\sim 22$  cm from ion and  $\beta$  implantation.

## 3 Results

A  $\gamma$ -ray energy-time matrix was produced for each Sm nucleus by placing a particle gate on the parent Pm nucleus. Four Pm nuclei were populated:  $^{160}\text{Pm}$ ,  $^{161}\text{Pm}$ ,  $^{162}\text{Pm}$ , and  $^{163}\text{Pm}$ . To study the  $\gamma$  rays in prompt coincidence with the  $\beta$  decay of the parent nucleus a short time gate of  $< 500$  ns was used. A time gate of  $\geq 500$  ns was used to investigate possible isomeric population following  $\beta$  decay. Four Pm isotopes were populated in this experiment, however the number of implanted  $^{163}\text{Pm}$  ions is much lower than the  $A = 160$ -162 nuclei and no  $\gamma$  rays were observed following the decay of this nucleus. Prompt coincident  $\gamma$  rays associated with the  $\beta$  decay of  $^{160}\text{Pm}$ ,  $^{161}\text{Pm}$ , and  $^{162}\text{Pm}$  can be seen in Fig. 1, Fig. 3, and Fig. 4 respectively.

### 3.1 $^{160}\text{Sm}$

Four  $\gamma$  rays of 108, 162, 250, and 1128 keV known to belong to the decay of  $^{160}\text{Sm}$  are seen in Fig. 1 [17, 18].

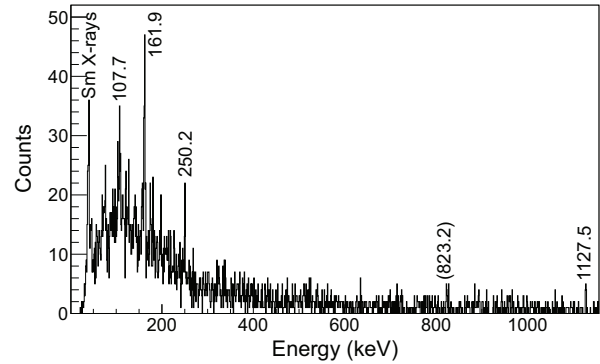


Figure 1. Energy spectrum of prompt  $\gamma$  rays in  $^{160}\text{Sm}$ .

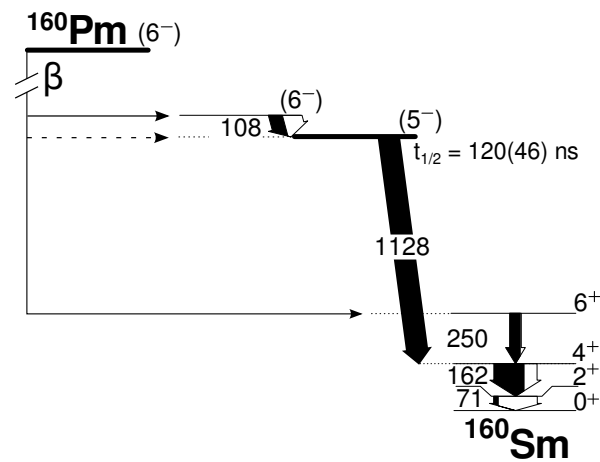


Figure 2. Level scheme of  $^{160}\text{Sm}$  populated by the  $\beta$  decay of  $^{160}\text{Pm}$ .

There is also a  $\gamma$ -ray peak visible at 823 keV, however, the origin of this  $\gamma$  ray is unknown. The 162 and 250 keV  $\gamma$  rays belong to the  $4^+ \rightarrow 2^+$  and  $6^+ \rightarrow 4^+$  transitions in the ground state band respectively. The 1128 keV  $\gamma$  ray is from the decay of a  $(5^-) \pi_{\frac{5}{2}}^- [532] \otimes \pi_{\frac{5}{2}}^+ [413]$  isomeric state [18] with a half-life of 120(46) ns [17]. The 108 keV  $\gamma$  ray originates from the  $(6^-)$  to  $(5^-)$  state transition [18].

The population of states in  $^{160}\text{Sm}$  via the  $\beta$  decay of  $^{160}\text{Pm}$  are shown in the level scheme in Fig. 2. The tentative assignment of a  $(6^-)$  spin-parity to the ground state of the parent nucleus is made on the basis that the  $\beta$  decay populates the  $(6^-)$  and  $6^+$  states in  $^{160}\text{Sm}$ . The intensities of the levels, measured in a 0 – 600 ns time window to include 5 half-lives of the isomeric state are shown in Tab. 1. The intensities balance through the levels within statistical uncertainties. It is likely that the  $\beta$  decay of  $^{160}\text{Pm}$  populates the  $(5^-)$  isomeric state directly, however there is no direct experimental evidence for this such as missing intensity, hence this transition is indicated by a dashed line in Fig. 2. Blocked BCS calculations presented in Table 3 also support a  $(6^-)$  spin-parity assignment of the  $^{160}\text{Pm}$  ground state.

**Table 1.** Initial level energy,  $E_i$  and spin-parity,  $J_i^\pi$  of the levels of  $^{160}\text{Sm}$  in this work. For each  $\gamma$  ray the energy,  $E_\gamma$ ,  $\gamma$ -ray intensity,  $I_\gamma$  relative to the 162-keV  $\gamma$ -ray intensity, and final level spin,  $J_f^\pi$ , are listed.

$E_i$ (keV)	$J_i^\pi$	$E_\gamma$ (keV)	$I_\gamma$ (rel.)	$J_f^\pi$
71(1)	(2 <sup>+</sup> )	71(1) <sup>a</sup>		0 <sup>+</sup>
233(1)	(4 <sup>+</sup> )	161.9(5)	100	(2 <sup>+</sup> )
483(1)	(6 <sup>+</sup> )	250.2(5)	35(18)	(4 <sup>+</sup> )
1361(1)	(5 <sup>-</sup> )	1127.5(5)	37(10)	(4 <sup>+</sup> )
1469(1)	(6 <sup>-</sup> )	107.7(8)	22(10)	(5 <sup>-</sup> )

<sup>a</sup> The 71-keV  $\gamma$  ray is only observed in coincident spectra.

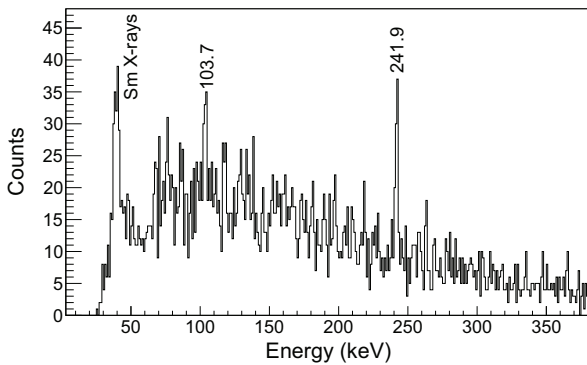


**Figure 3.** Energy spectrum of prompt  $\gamma$  rays in  $^{161}\text{Sm}$ .

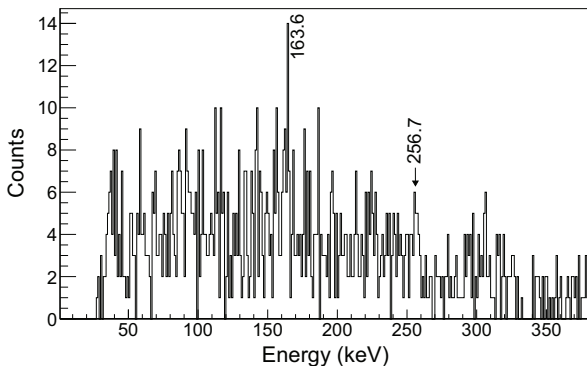


**Figure 4.** Energy spectrum of prompt  $\gamma$  rays in  $^{162}\text{Sm}$ .

### 3.2 $^{161}\text{Sm}$

Two  $\gamma$  rays of 104- and 242-keV energy are seen in prompt coincidence with the  $\beta$  decay of  $^{161}\text{Pm}$ , shown in Fig. 3. They do not appear in coincidence with each other, or in a delayed  $\beta - \gamma$  coincident spectrum, therefore it is likely they belong to two different bands, each populated directly by  $\beta$  decay. Blocked BCS calculations presented in Section 4.2 show several possibilities for the spin-parities of the states in  $^{161}\text{Pm}$  and  $^{161}\text{Sm}$ .

### 3.3 $^{162}\text{Sm}$

Two  $\gamma$  rays are visible in prompt coincidence with the  $\beta$  decay of  $^{162}\text{Pm}$  into  $^{162}\text{Sm}$ . From systematics of neighbouring nuclei it is likely that the 164-keV  $\gamma$  ray is from

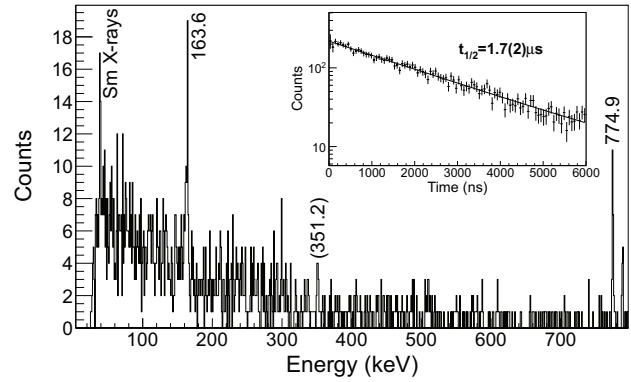


**Figure 5.**  $\beta$ -delayed  $\gamma$  energy spectrum of  $^{162}\text{Sm}$  with  $t \geq 500$  ns. A 789-keV  $\gamma$  ray from the self activity in the  $\text{LaBr}_3(\text{Ce})$  detectors added to EURICA is also visible. Inset: The exponential decay curve is from the isomeric decay of  $^{162}\text{Sm}$ , found using the passive stopper part of the experiment.

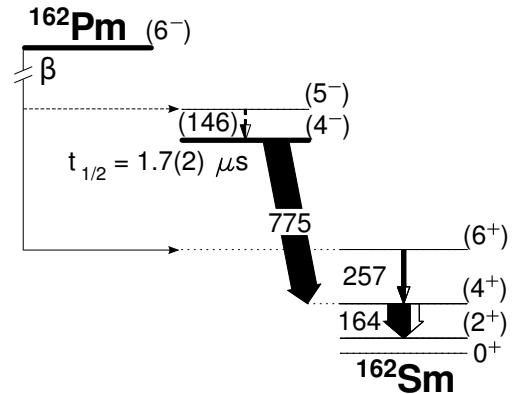


**Figure 6.** Level scheme of  $^{162}\text{Sm}$  populated by the  $\beta$  decay of  $^{162}\text{Pm}$ .

**Table 2.** Initial level energy,  $E_i$  and spin-parity,  $J_i^\pi$  of the levels of  $^{162}\text{Sm}$  in this work. For each  $\gamma$  ray the energy,  $E_\gamma$ ,  $\gamma$ -ray intensity,  $I_\gamma$  relative to the 775-keV  $\gamma$ -ray intensity, and final level spin,  $J_f^\pi$ , are listed.

$E_i - E(2^+)$ (keV)	$J_i^\pi$	$E_\gamma$ (keV)	$I_\gamma$ (rel.)	$J_f^\pi$
163.6(7)	(4 <sup>+</sup> )	163.6(7)	87(29)	(2 <sup>+</sup> )
420(1)	(6 <sup>+</sup> )	256.7(9)	15(3)	(4 <sup>+</sup> )
938.5(8)	(4 <sup>-</sup> )	774.9(5)	100	(4 <sup>+</sup> )
1085(1)	(5 <sup>-</sup> )	146(1) <sup>a</sup>		(4 <sup>-</sup> )

<sup>a</sup> The 146-keV  $\gamma$  ray is only observed in coincident spectra.

the 4<sup>+</sup>  $\rightarrow$  2<sup>+</sup> transition and the 257-keV  $\gamma$  ray is from the 6<sup>+</sup>  $\rightarrow$  4<sup>+</sup> transition. The 2<sup>+</sup>  $\rightarrow$  0<sup>+</sup> transition is expected to be around 70 keV from systematics. It was not observed due to the high internal conversion rate expected for this low energy transition.

An isomeric state in  $^{162}\text{Sm}$  is populated via  $\beta$  decay, shown in the  $\beta$ -delayed coincident  $\gamma$ -ray spectrum in Fig. 5. A 775-keV  $\gamma$  ray appears and the 257-keV  $\gamma$  ray is no longer visible in the delayed  $\gamma$ -ray spectrum which suggests the  $\beta$  decay populates an isomeric state of  $^{162}\text{Sm}$  with

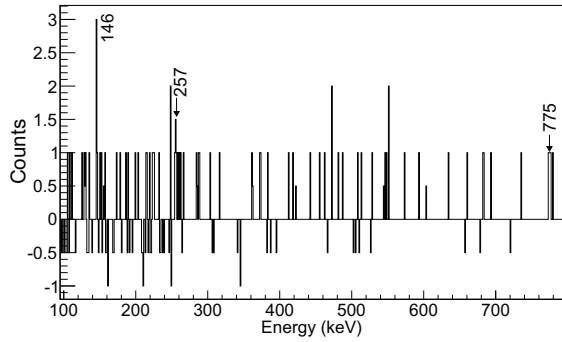


**Figure 7.**  $\gamma$ -ray spectrum gated on the 164-keV  $\gamma$  ray. A 146-keV  $\gamma$  ray is visible in addition to the 257 and 775 keV  $\gamma$  rays.

a half-life longer than 500 ns in addition to the ( $6^+$ ) state in the ground band. The 775-keV transition directly feeds the 164-keV transition, therefore it populates the ( $4^+$ ) ground band state. The spin-parity of the isomeric state is assigned as ( $4^-$ ) based on a lack of transitions to the ( $2^+$ ) and ( $6^+$ ) ground band states. This is supported by blocked BCS calculations presented in Table 4. The level scheme of  $^{162}\text{Sm}$  is shown in Fig. 6. The intensities of the  $\gamma$  rays, shown in Table 2, are calculated at  $t = 0$  using the exponential law of radioactive decay,  $N(t) = N_0 e^{(-\lambda t)}$ , in order to compare the intensities of the isomer-delayed  $\gamma$  rays to the intensities of the prompt  $\gamma$  rays.

The spin-parity of the ground state in the parent nucleus,  $^{162}\text{Pm}$ , is assigned ( $6^-$ ) due to the decay to the ( $6^+$ ) ground band state, similar to  $^{160}\text{Sm}$ . Blocked BCS calculations in Table 3 support this assignment. However, the ( $6^-$ ) state in  $^{162}\text{Pm}$  is strongly forbidden to decay into the ( $4^-$ ) isomeric state in  $^{162}\text{Sm}$  due to the  $\Delta I = 2$  and parity change required. Therefore it is likely that the  $^{162}\text{Pm}$  ground state decays into a level on top of the isomeric state. Indeed, a 146-keV  $\gamma$  ray is visible in a background subtracted 164-keV coincidence spectrum, shown in Fig. 7. This  $\gamma$  ray is tentatively placed as a transition from a ( $5^-$ ) state to the isomeric ( $4^-$ ) state in Fig. 6.

These Sm nuclei were also produced directly in the fission reaction at the start of BigRIPS. In order to study isomers in these nuclei a passive stopper was used in place of WAS3ABi, which allowed for a higher implantation rate. The experimental set-up is detailed in [8, 19]. The ( $4^-$ ) isomeric state in  $^{162}\text{Sm}$  was also observed in this passive stopper part of the experiment, with a measured high-precision half-life of 1.7(2)  $\mu\text{s}$  [19], seen in Fig. 5.

## 4 Discussion

Blocked BCS calculations of the type in Ref. [20] were performed in order to better understand the spin-parities of the ground states in  $^{160}\text{Pm}$ ,  $^{161}\text{Pm}$ , and  $^{162}\text{Pm}$ , and to understand the spin-parity of the isomeric state in  $^{162}\text{Sm}$ . The pairing strengths were fixed as  $G_\pi = 21.0$  A-MeV and  $G_\nu = 20.0$  A-MeV, in accordance with Jain *et al.* [20], and the deformation parameters were taken from Möller *et al.* [21]. The results can be seen in Table 3 and Table 4.

**Table 3.** Low-lying quasiparticle states in  $^{160}\text{Pm}$ ,  $^{161}\text{Pm}$ , and  $^{162}\text{Pm}$  predicted by blocked-BCS calculations. Only  $K^\pi$  values of favoured spin-couplings are shown.

Nucleus	$K^\pi$	Configuration	$E_x$ (keV)
$^{160}\text{Pm}$	$6^-$	$\nu_{7/2}^{7+}[633] \otimes \pi_{5/2}^{5-}[532]$	0
$^{160}\text{Pm}$	$2^+$	$\nu_{7/2}^{1-}[521] \otimes \pi_{5/2}^{5-}[532]$	52
$^{160}\text{Pm}$	$3^-$	$\nu_{7/2}^{1-}[521] \otimes \pi_{5/2}^{5+}[413]$	289
$^{160}\text{Pm}$	$5^+$	$\nu_{7/2}^{5-}[512] \otimes \pi_{5/2}^{5-}[532]$	436
$^{161}\text{Pm}$	$5^-$	$\pi_{5/2}^{5-}[532]$	0
$^{161}\text{Pm}$	$5^+$	$\pi_{5/2}^{5+}[413]$	268
$^{161}\text{Pm}$	$3^+$	$\pi_{3/2}^{3+}[411]$	586
$^{161}\text{Pm}$	$3^-$	$\pi_{3/2}^{3-}[541]$	672
$^{162}\text{Pm}$	$2^+$	$\nu_{7/2}^{1-}[521] \otimes \pi_{5/2}^{5-}[532]$	0
$^{162}\text{Pm}$	$6^-$	$\nu_{7/2}^{7+}[633] \otimes \pi_{5/2}^{5-}[532]$	44
$^{162}\text{Pm}$	$5^+$	$\nu_{7/2}^{5-}[512] \otimes \pi_{5/2}^{5-}[532]$	163
$^{162}\text{Pm}$	$3^-$	$\nu_{7/2}^{1-}[521] \otimes \pi_{5/2}^{5-}[413]$	196

### 4.1 $^{160}\text{Sm}$

The lowest energy configuration for the ground state of  $^{160}\text{Pm}$  from blocked BCS calculations presented in Table 3 is  $6^- \nu_{7/2}^{7+}[633] \otimes \pi_{5/2}^{5-}[532]$ . This supports the assignment made in Section 3.1. The ground state of  $^{160}\text{Pm}$  is assigned a ( $6^-$ ) spin-parity that  $\beta$  decays to the ( $6^-$ ) and ( $6^+$ ) states in  $^{160}\text{Sm}$ . A  $2^+ \nu_{7/2}^{1-}[521] \otimes \pi_{5/2}^{5-}[532]$  configuration is also predicted by the calculations to have low energy. It is possible that a second state with  $2^+$  spin-parity exists in  $^{160}\text{Pm}$  that decays to the  $2^+$  ground band state in  $^{160}\text{Sm}$ , however, due to lack of experimental evidence the  $2^+$  state in  $^{160}\text{Pm}$  has not been placed in the level scheme. The reduced hindrance of the 1128-keV transition depopulating the  $5^-$  isomer is  $f_\nu \sim 20$ . The reduced hindrances of the two known K isomers in  $^{160}\text{Sm}$  are discussed in detail in reference [18].

### 4.2 $^{161}\text{Sm}$

Blocked BCS calculations display many possible ground state configurations of  $^{161}\text{Pm}$  shown in Table 3. The calculations also reveal many possible low-lying states in  $^{161}\text{Sm}$ . The two  $\gamma$  rays in the energy spectrum of  $^{161}\text{Sm}$  are not in coincidence with each other. It is possible that they arise from the  $\beta$  decay of two different states in  $^{161}\text{Pm}$  into a single state in  $^{161}\text{Sm}$ . It is also possible that they are both populated from the  $\beta$  decay of one state in  $^{161}\text{Pm}$  into two different states in  $^{161}\text{Sm}$ . Therefore it is not possible to determine the decay pattern or to assign spin-parities to these possible states.

### 4.3 $^{162}\text{Sm}$

The blocked BCS calculations for the ground state of  $^{162}\text{Pm}$  show a similar result to the calculations for  $^{160}\text{Pm}$ . A  $2^+ \nu_{7/2}^{1-}[521] \otimes \pi_{5/2}^{5-}[532]$  configuration is lowest in energy, followed by a  $6^- \nu_{7/2}^{7+}[633] \otimes \pi_{5/2}^{5-}[532]$  configuration

**Table 4.** Low-lying quasiparticle states in  $^{162}\text{Sm}$  predicted by blocked-BCS calculations.

$K^\pi$	configuration	$E_x$ (MeV)
$5^-$	$\pi_{\frac{5}{2}}^{-}[532] \otimes \pi_{\frac{5}{2}}^{-}[413]$	1.000
$4^-$	$\nu_{\frac{7}{2}}^{+}[633] \otimes \nu_{\frac{1}{2}}^{-}[521]$	1.043
$4^-$	$\pi_{\frac{5}{2}}^{-}[532] \otimes \pi_{\frac{3}{2}}^{+}[411]$	1.547 <sup>(a)</sup>
$4^+$	$\pi_{\frac{5}{2}}^{-}[413] \otimes \pi_{\frac{3}{2}}^{+}[411]$	1.614
$3^+$	$\nu_{\frac{1}{2}}^{-}[521] \otimes \nu_{\frac{5}{2}}^{-}[512]$	1.668
$6^-$	$\nu_{\frac{7}{2}}^{+}[633] \otimes \nu_{\frac{5}{2}}^{-}[512]$	1.797 <sup>(a)</sup>

<sup>a</sup> 200 keV has been added to these states as they have energetically unfavoured configurations according to the residual spin-spin coupling rule.

only 44 keV apart. The ground state in  $^{162}\text{Pm}$  is assigned a ( $6^-$ ) spin-parity due to population of the ( $6^+$ ) ground band state in  $^{162}\text{Sm}$ . The 257-keV transition from the ( $6^+$ ) state is weakly populated compared to the isomeric state, therefore it is determined to be a forbidden transition. The decay to the ( $5^-$ ) state on top of the isomeric state is allowed. It is possible that a second ground state in  $^{162}\text{Pm}$  exists with a spin-parity of  $2^+$  as in  $^{160}\text{Pm}$ , however experimental evidence is not present. If it exists it would decay into the ( $2^+$ ) ground band state in  $^{162}\text{Sm}$ .

The lowest energy quasiparticle configurations in  $^{162}\text{Sm}$  predicted by blocked BCS calculations are a  $5^- \pi_{\frac{5}{2}}^{-}[532] \otimes \pi_{\frac{5}{2}}^{-}[413]$  configuration and a  $4^- \nu_{\frac{7}{2}}^{+}[633] \otimes \nu_{\frac{1}{2}}^{-}[521]$  that are only 43 keV apart. The isomeric state in  $^{162}\text{Sm}$  is assigned a ( $4^-$ ) spin-parity based on the lack of observation of a transition from the isomeric state to the ( $6^+$ ) state. If such a transition existed it would be visible in the  $\gamma$ -ray spectrum. This assignment is also supported by the calculations presented in Table 4.

The reduced hindrance of the 775-keV transition depopulating the  $4^-$  isomer is  $f_v \sim 70$ . This is larger than in  $^{160}\text{Sm}$ , but consistent with the limit found for the  $4^-$  isomer in  $^{154}\text{Nd}$  [17].

## 5 Conclusions

Low-lying states in  $^{160}\text{Sm}$ ,  $^{161}\text{Sm}$ , and  $^{162}\text{Sm}$  were populated via  $\beta$  decay for the first time. Isomeric states in  $^{160}\text{Sm}$  and  $^{162}\text{Sm}$  were also observed following  $\beta$  decay, assigned a ( $5^-$ )  $\pi_{\frac{5}{2}}^{-}[532] \otimes \pi_{\frac{5}{2}}^{-}[413]$  [18] and a ( $4^-$ )  $\nu_{\frac{7}{2}}^{+}[633] \otimes \nu_{\frac{1}{2}}^{-}[521]$  configuration respectively. The ground states in  $^{160}\text{Pm}$  and  $^{162}\text{Pm}$  were determined to have a ( $6^-$ )  $\nu_{\frac{7}{2}}^{+}[633] \otimes \pi_{\frac{5}{2}}^{-}[532]$  configuration. Further experimental evidence is required to determine the ground state of  $^{161}\text{Pm}$ . Further work is also required to extract the  $\beta$  decay half-life and the  $Q_\beta$  values of the parent nuclei  $^{160}\text{Pm}$ ,  $^{161}\text{Pm}$ , and  $^{162}\text{Pm}$ .

## Acknowledgements

This work was carried out at the RIBF operated by RIKEN Nishina Center, RIKEN and CNS, University of Tokyo.

All UK authors are supported by STFC. P. H. R. and G. L. are partially supported by the UK National Measurement Office (NMO). P.-A. S. was financed by JSPS Grant Number 23.01752 and the RIKEN Foreign Postdoctoral Researcher Program. J. T. was financed by Spanish Ministerio de Ciencia e Innovación under Contracts No. FPA2009-13377-C02 and No. FPA2011-29854-C04. Zs. D., I. K., and Zs. V. were supported by OTKA contract number K100835. We acknowledge the EUROBALL Owners Committee for the loan of germanium detectors and the PreSpec Collaboration for the readout electronics of the cluster detectors. This work was supported by JSPS KAKENHI Grant No. 25247045.

## References

- [1] E. M. Burbidge, G. R. Burbidge, W. A. Fowler *et al.*, *Rev. Mod. Phys.* **29**, 547 (1957).
- [2] J. A. Winger, S. V. Ilyushkin, K. P. Rykaczewski *et al.*, *Phys. Rev. Lett.* **102**, 142502 (2009).
- [3] A. Jungclauss, L. Cáceres, M. Górska *et al.*, *Phys. Rev. Lett.* **99**, 132501 (2007).
- [4] A. I. Morales, J. Benlliure, T. Kurtukián-Nieto *et al.*, *Phys. Rev. Lett.* **113**, 022702 (2014).
- [5] R. Surman, J. Engel, J. R. Bennett *et al.*, *Phys. Rev. Lett.* **79**, 1809 (1997).
- [6] S. K. Ghorui, B. B. Sahu, C. R. Praharaaj *et al.*, *Phys. Rev. C* **85**, 064327 (2012).
- [7] S. K. Ghorui (2014), private communication
- [8] Z. Patel, P. A. Söderström, Z. Podolyák *et al.*, *Phys. Rev. Lett.* **113**, 262502 (2014).
- [9] Y. Yano, *Nucl. Instrum. Meth. B* **261**, 1009 (2007).
- [10] T. Kubo, D. Kameda, H. Suzuki *et al.*, *Prog. Theor. Exp. Phys.* p. 03C003 (2012).
- [11] T. Kubo, D. Kameda, H. Suzuki *et al.*, *Prog. Theor. Exp. Phys.* p. 03C003 (2012).
- [12] Y. Yano, *Nucl. Instrum. Meth. B* **261**, 1009 (2007).
- [13] S. Nishimura, G. Lorusso, Z. Xu *et al.*, *RIKEN Accel. Prog. Rep.* **46**, 182 (2013).
- [14] S. Nishimura, *Nucl. Phys. News Int.* **22**, 38 (2012).
- [15] P. A. Söderström, S. Nishimura, P. Doornenbal *et al.*, *Nucl. Instrum. Meth. B* **317**, 649 (2013).
- [16] P. A. Söderström, S. Nishimura, P. Doornenbal *et al.*, *Nucl. Instrum. Meth. B* **317**, 649 (2013).
- [17] G. S. Simpson, W. Urban, J. Genevey *et al.*, *Phys. Rev. C* **80**, 024304 (2009).
- [18] Z. Patel, Z. Podolyák, P. Walker *et al.*, *Phys. Lett. B* **753**, 182 (2016).
- [19] Z. Patel, Ph.D. thesis, The University of Surrey (2015).
- [20] K. Jain, O. Burglin, G. Dracoulis *et al.*, *Nucl. Phys.* **A591**, 61 (1995).
- [21] P. Möller, J. Nix, W. Myers *et al.*, *Atom. Data Nucl. Data* **59**, 185 (1995).